Connecting dark matter to galaxies

- halo abundance matching

Halo Abundance matching

- rank galaxies by stellar mass
- rank halos and sub halos by halo mass or by circular velocity
- starting with the most massive objects assign most massive galaxy to the most massive halo; the second massive galaxy to the second massive halo and so on

This provides mapping of galaxies to DM halos.

The process involves *lots* of minute details, but works remarkably well. It cannot be absolutely correct (neglects the history of star formation for a change).

Main assumption is that the mass of DM halo defines stellar mass. Everything else plays secondary roles.

Clustering: DM halos and L

Conroy, Wechsler, Kravtsov (2005): **N-body only**

- Get all halos from high-res simulation
- Use maximum circular velocity (NOT mass)
- For subhalos use V_{max} before they became subhalos
- Every halo (or subhalo) is a galaxy
- Every halo has luminosity: **LF is as in SDSS**
- No cooling or major mergers and such. Only DM halos

Reproduces most of the observed clustering of galaxies

SDSS: z=0

DM galaxies

DM

SDSS

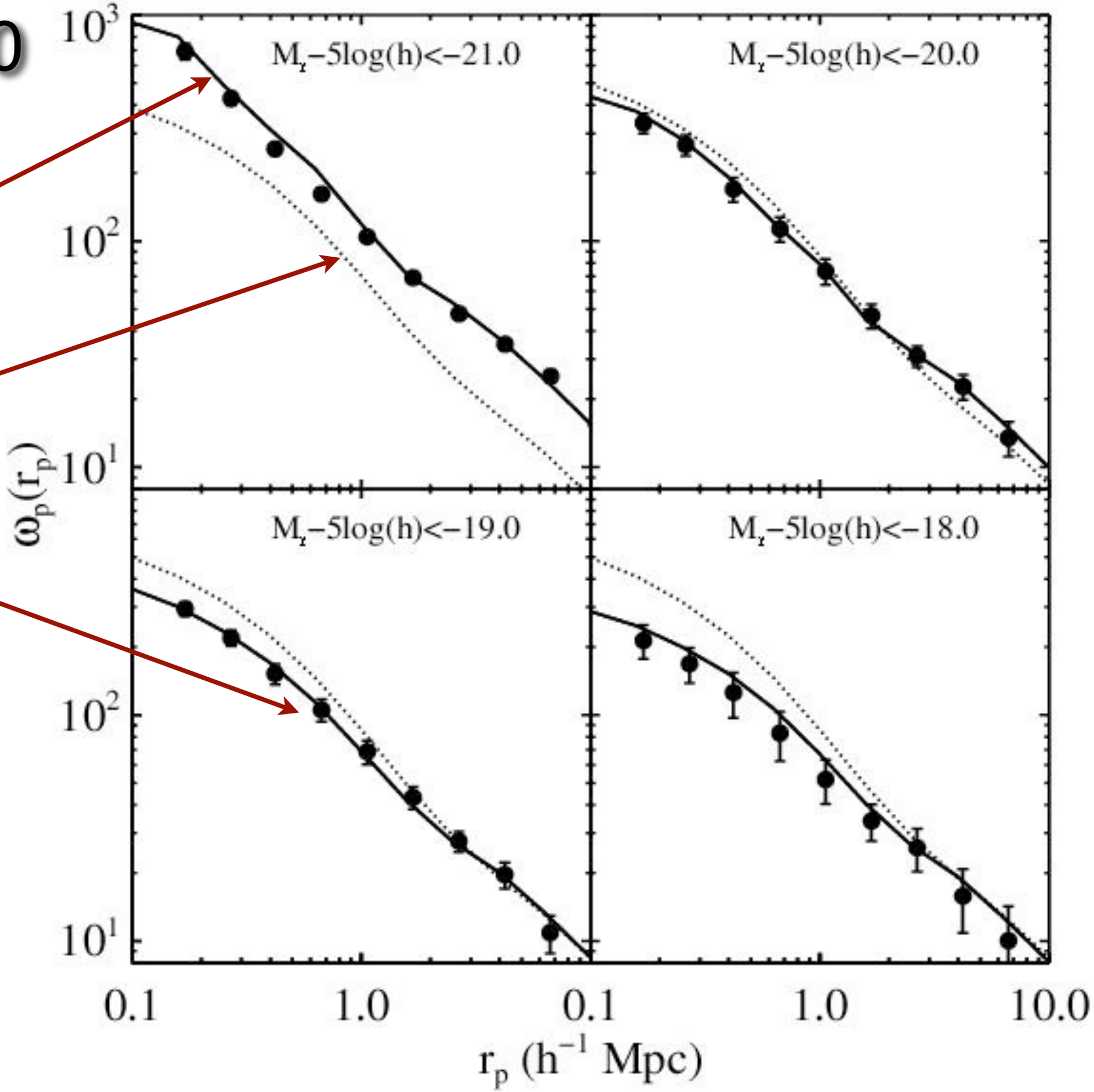

Why it works.

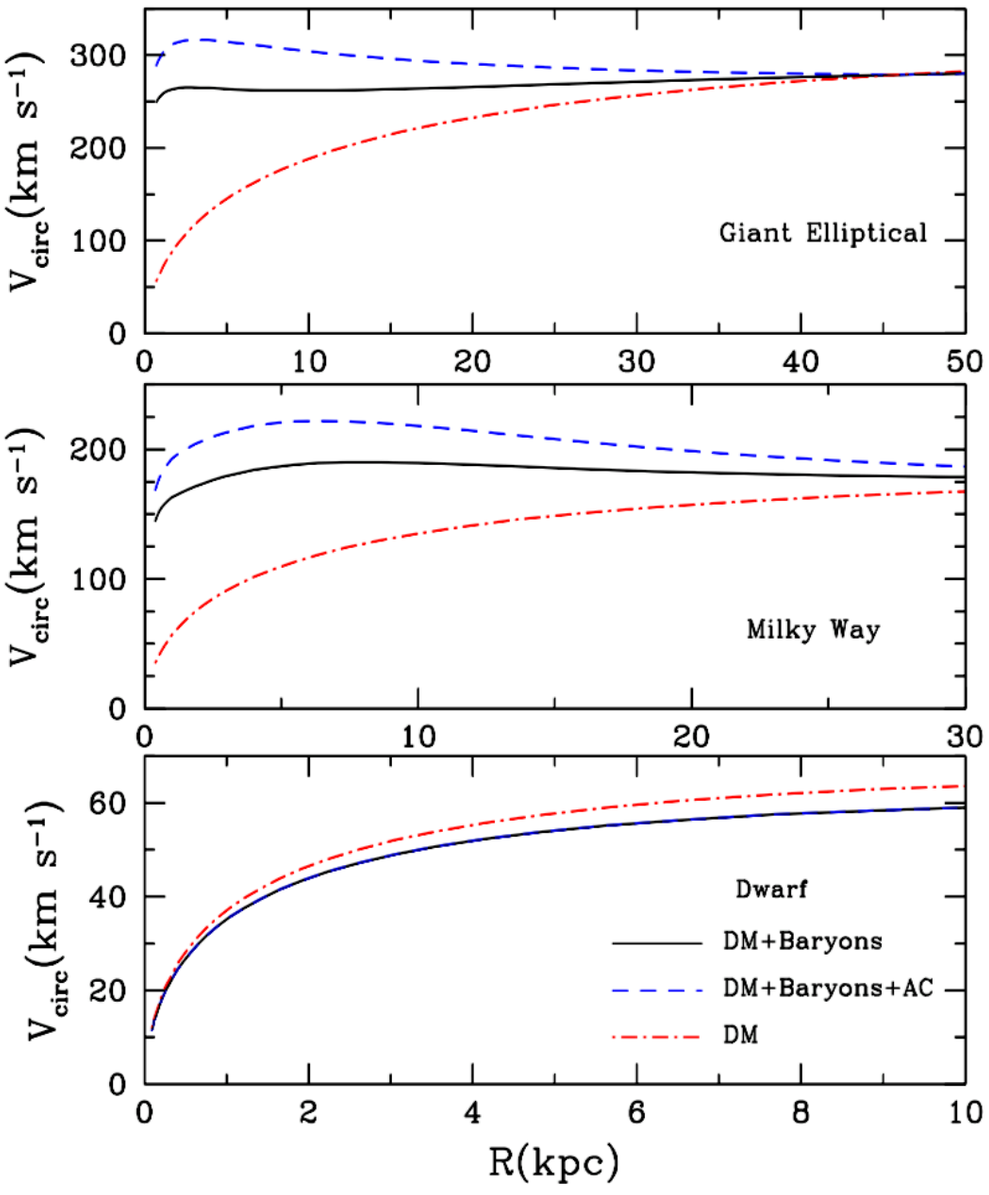

Flat circular velocity curves for galaxies. Simple analytical models of dark matter profiles with stellar +gas components. Central regions may be dominated by baryons, but the the outer parts are DM dominated and both have the SAME circular velocities.

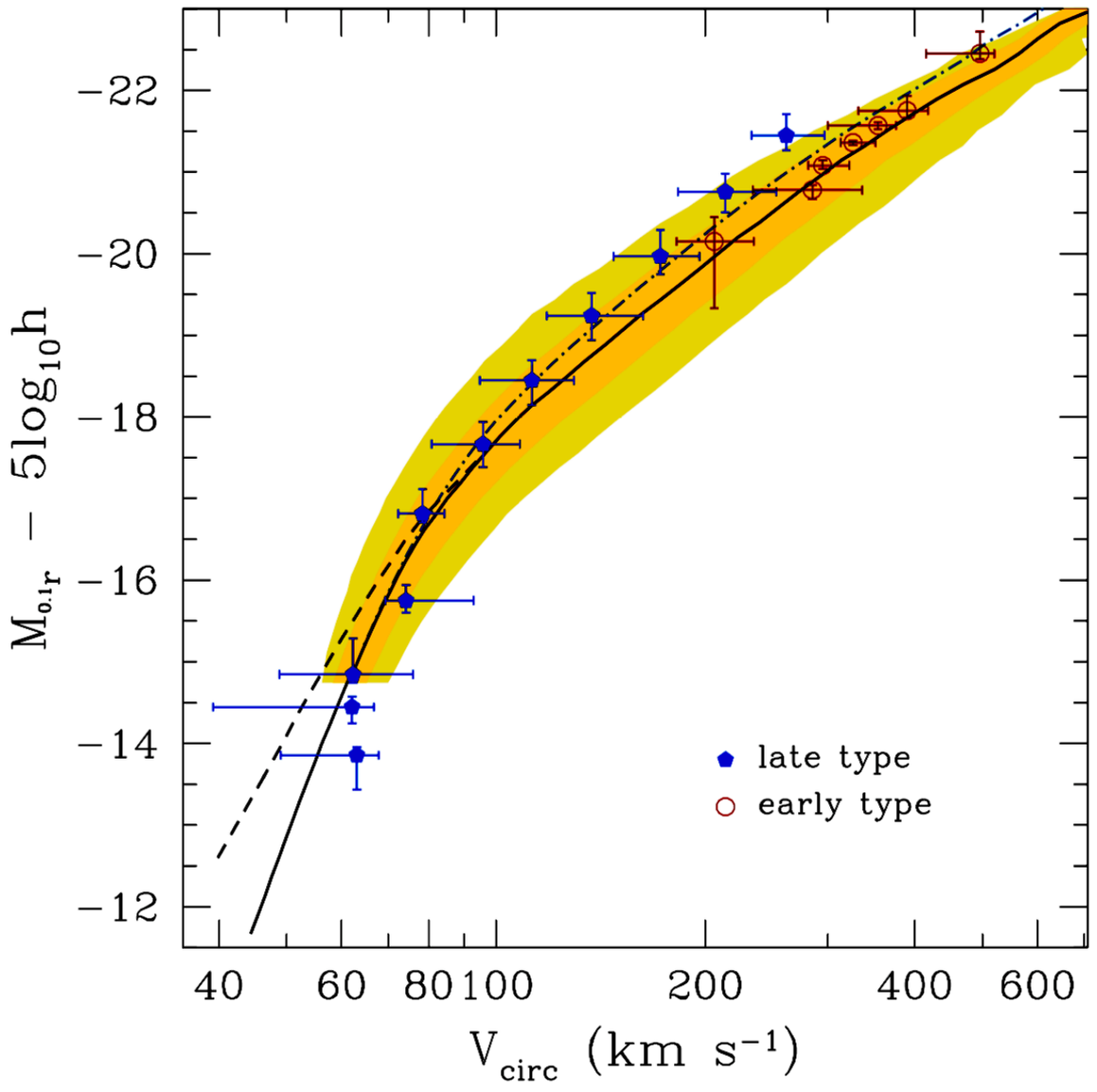

Comparison of the observed Luminosity-Velocity relation with the predictions of the ΛCDM model using halo abundance matching. The solid curve shows the median values of 0.1r-band luminosity vs. circular velocity for the model galaxy sample.

Trujillo-Gomez et al 2011

BTFR (blue) and Mhalo – Vflat relation (green) for the Flat Rotation curve model.

Data are for HI measured rotation curves.

Halo masses are based on rotation curves in Di Cintio & Brook (2014) cosmological simulations

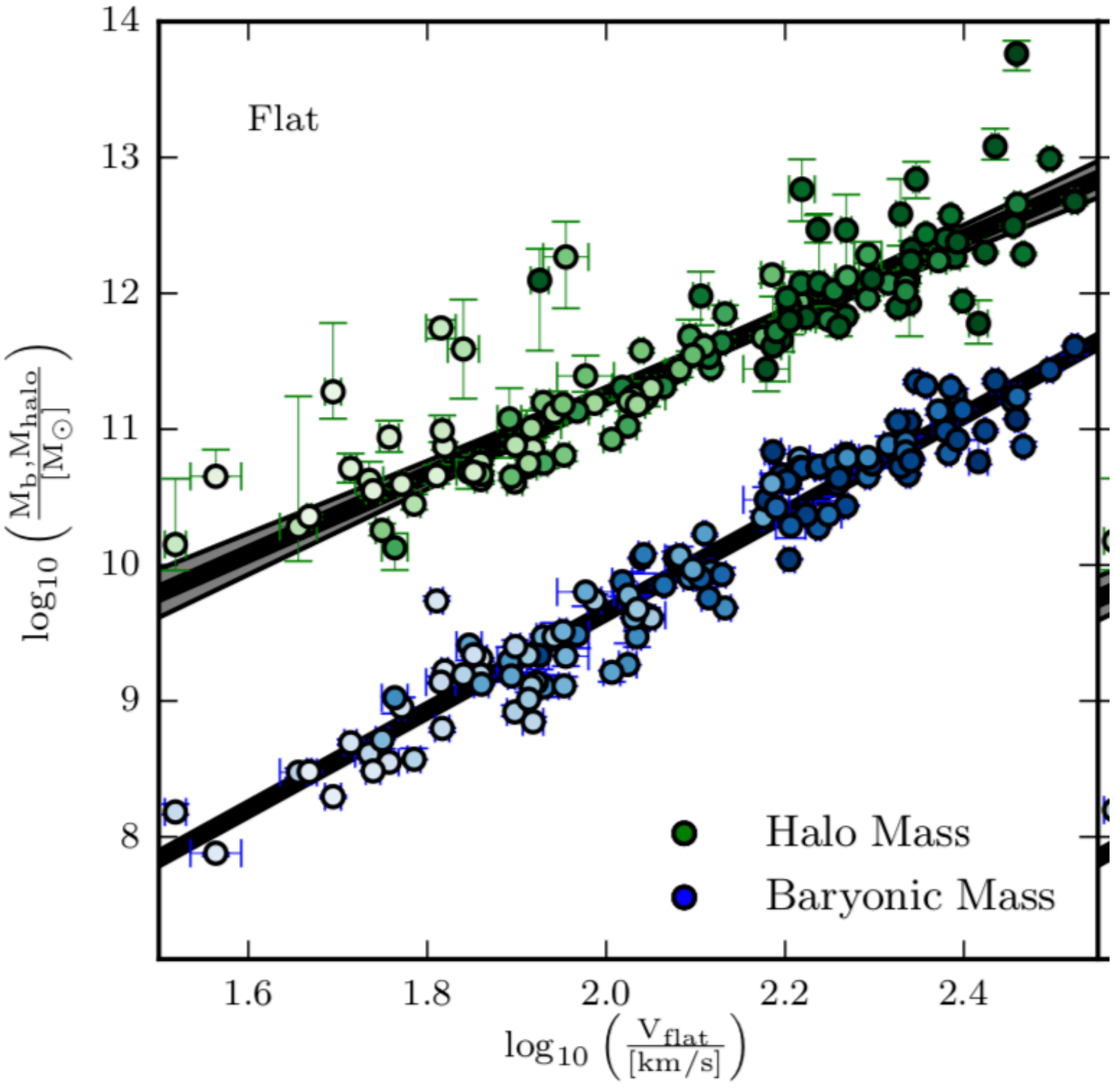

Katz et al 2018

Halo Abundance matching

Input from observations: stellar mass function at different redshifts

Input from theory: (sub)halo velocity function or (sub)halo mass function

Behroozi et al 2013

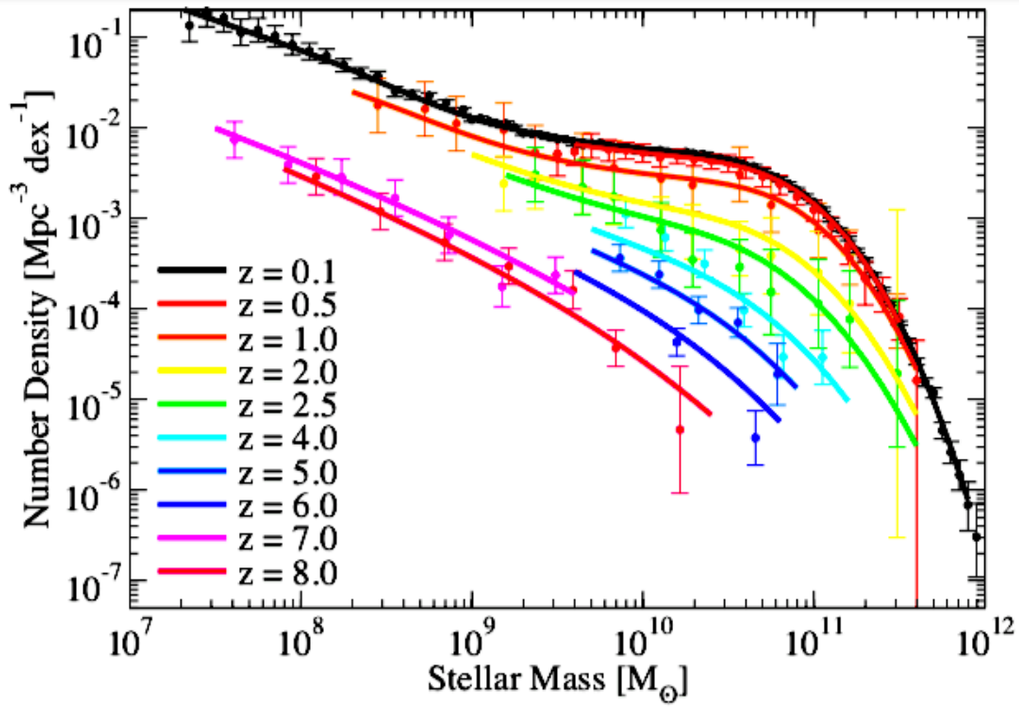

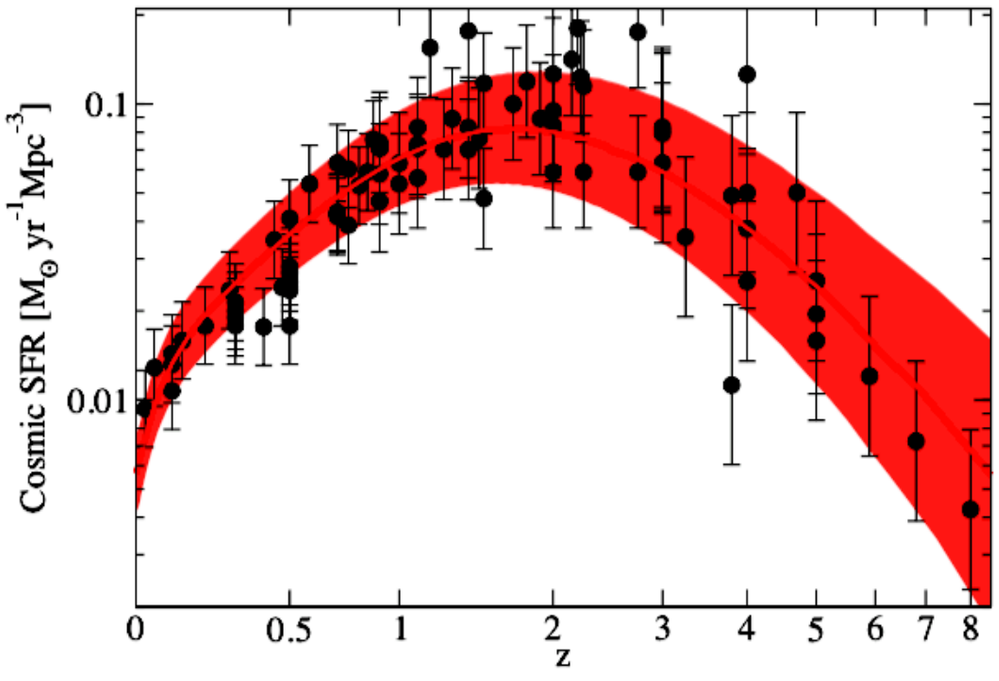

FIG. 3.— **Top** panel: Evolution of the stellar mass function from $z = 0$ to $z = 8$ in the best fitting model (colored lines), compared to observations (points with error bars; for clarity not all data is shown). **Bottom** panel: Observational constraints on the cosmic star formation rate (black points), compared to the best-fit model (red solid line) and the posterior one-sigma distribution (red shaded region).

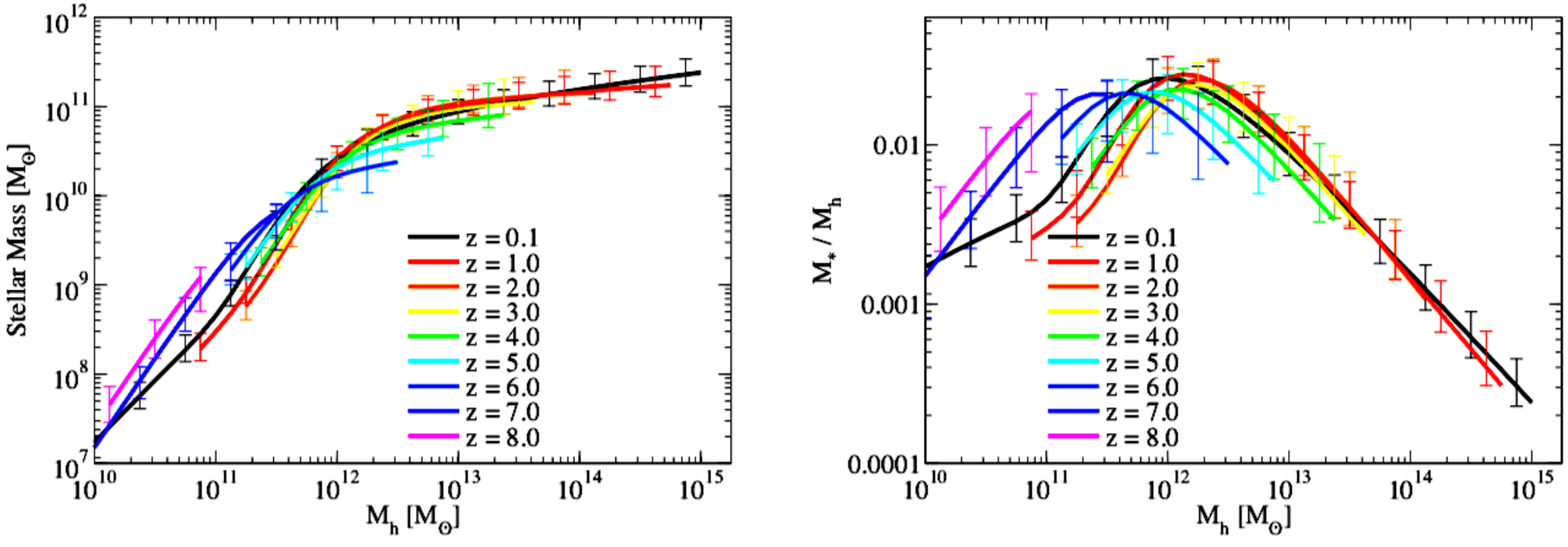

FIG. 7.— **Left** panel: Evolution of the derived stellar mass as a function of halo mass. In each case, the lines show the mean values for central galaxies. These relations also characterize the satellite galaxy population if the horizontal axis is interpreted as the halo mass at the time of accretion. Error bars include both systematic and statistical uncertainties, calculated for a fixed cosmological model (see §4 for details). **Right** panel: Evolution of the derived stellar mass fractions (M_*/M_h) as a function of halo mass.

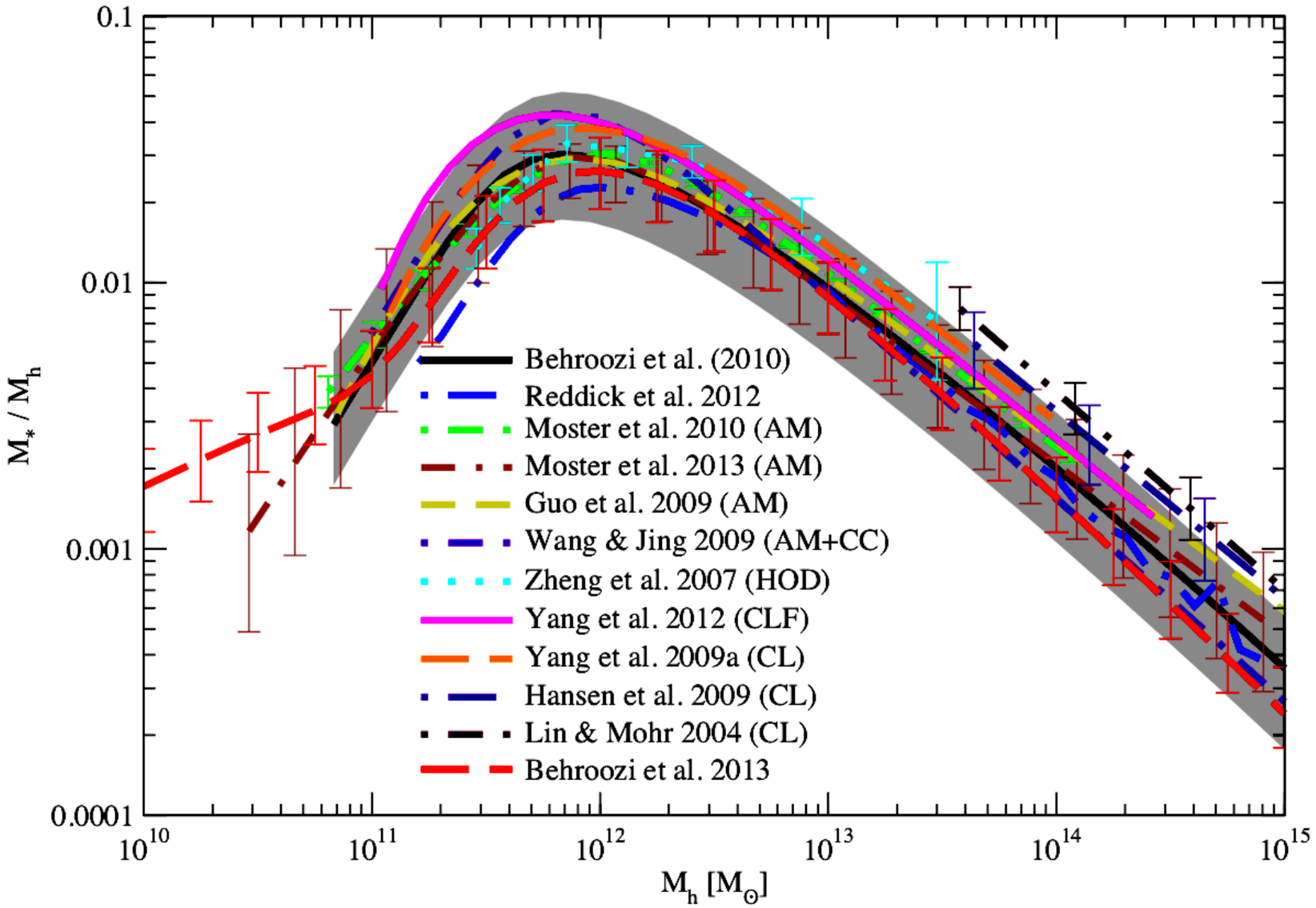

FIG. 14.— Comparison of our best-fit model at $z = 0.1$ to previously published results. Results compared include those from our previous work (Behroozi et al. 2010), from abundance matching (Moster et al. 2013; Reddick et al. 2012; Moster et al. 2010; Guo et al. 2010; Wang & Jing 2010), from HOD/CLF modeling (Zheng et al. 2007a; Yang et al. 2012), and from cluster catalogs (Yang et al. 2009a; Hansen et al. 2009; Lin & Mohr 2004). Grey shaded regions correspond to the 68% confidence contours of Behroozi et al. (2010). The one-sigma posterior distribution for our model is shown by the red error bars.

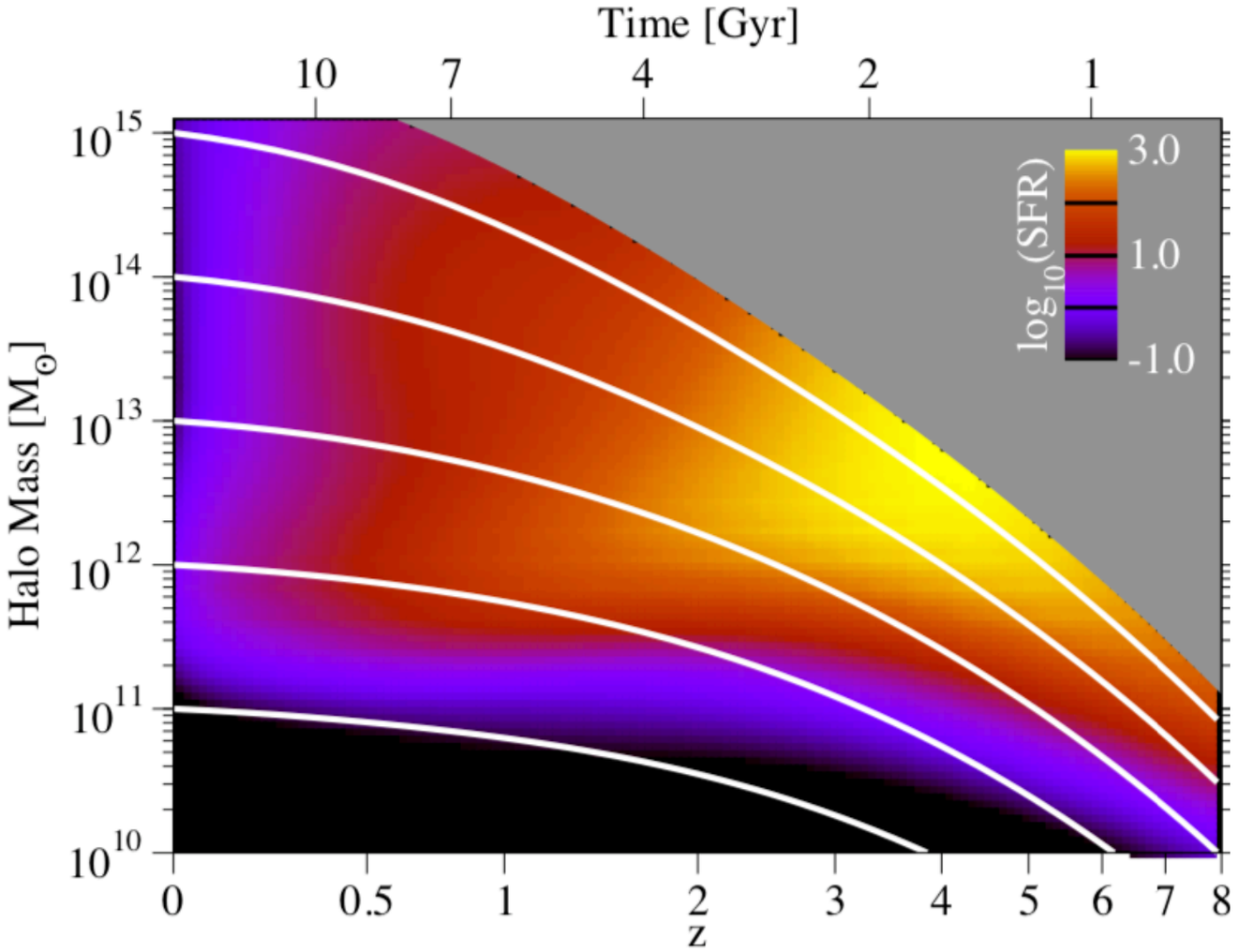

Average star formation rates as a function of halo mass and redshift. The overlaid white lines show average mass accretion histories for halos as a function of redshift for comparison.

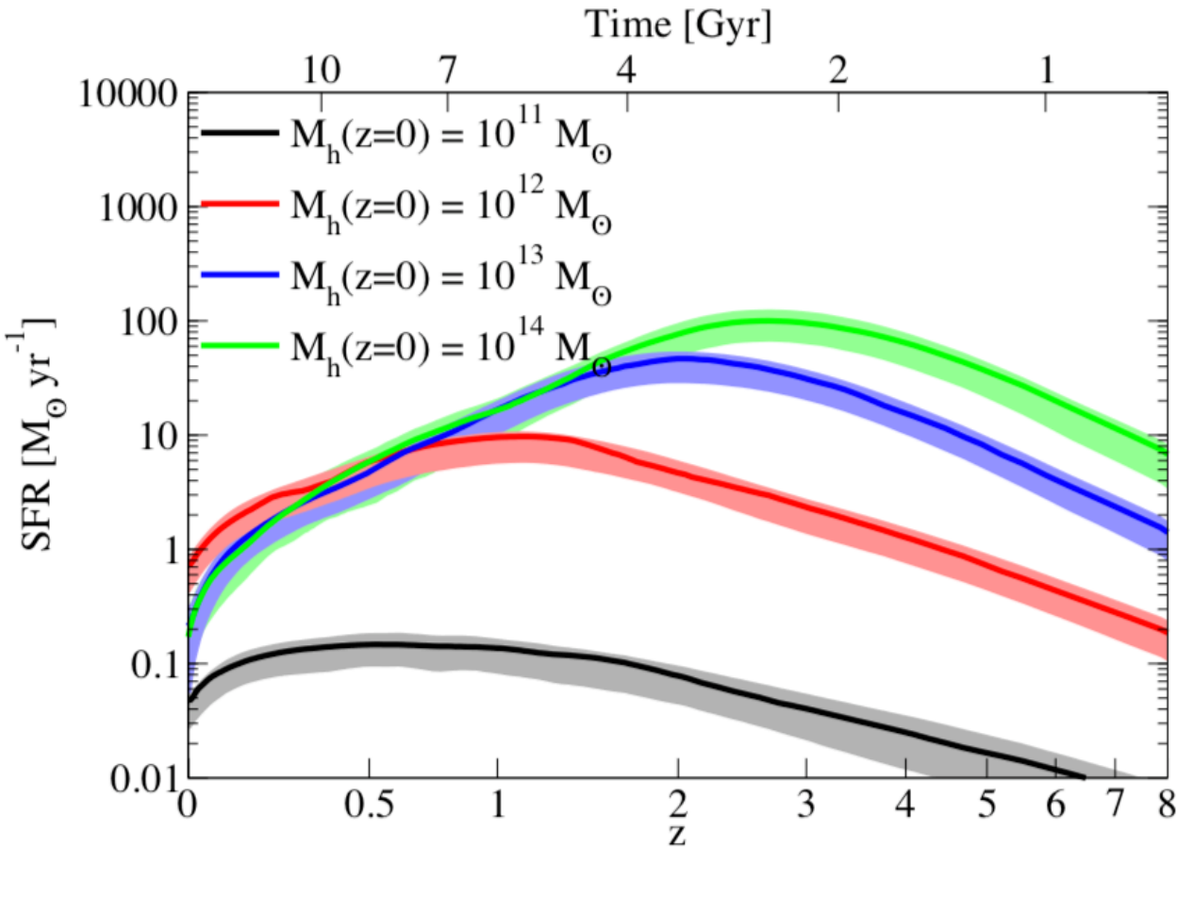

Average star formation histories as a function of halo mass and redshift (lines).

Halo Abundance matching: application to BOSS CMASS sample z=0.5

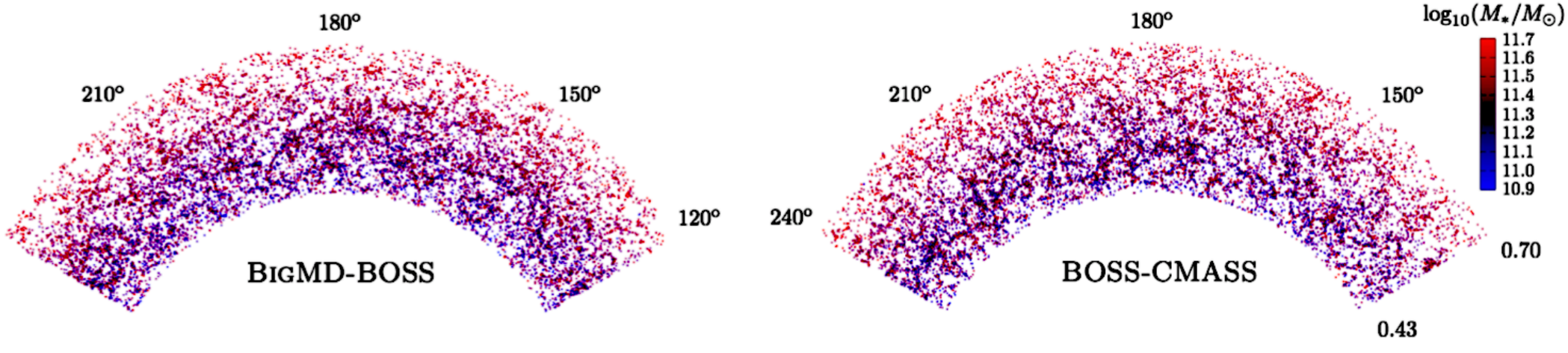

The Baryon Oscillations Spectroscopic Survey (BOSS): 1.5 million galaxies

10,000 deg2 divided into two samples: LOWZ and CMASS. The LOWZ galaxies are selected to be the brightest and reddest of the low- redshift galaxy population (z <0.4), extending the SDSS I/II LRGs. The CMASS target selection is designed to isolate galaxies at higher redshift (z > 0.4), most of them being also luminous red galaxies.

Sergio A. Rodr´ıguez-Torres et al. 2016

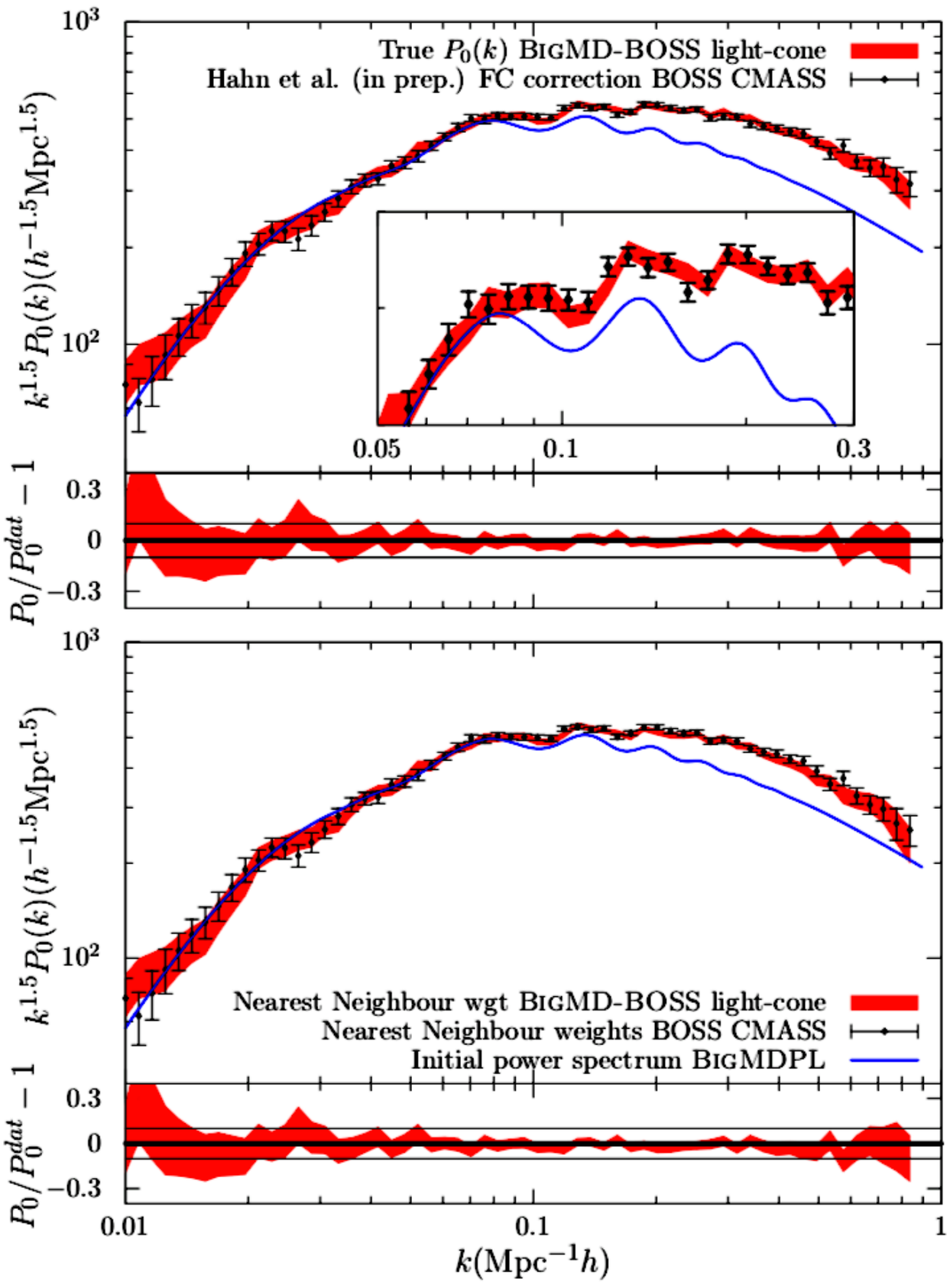

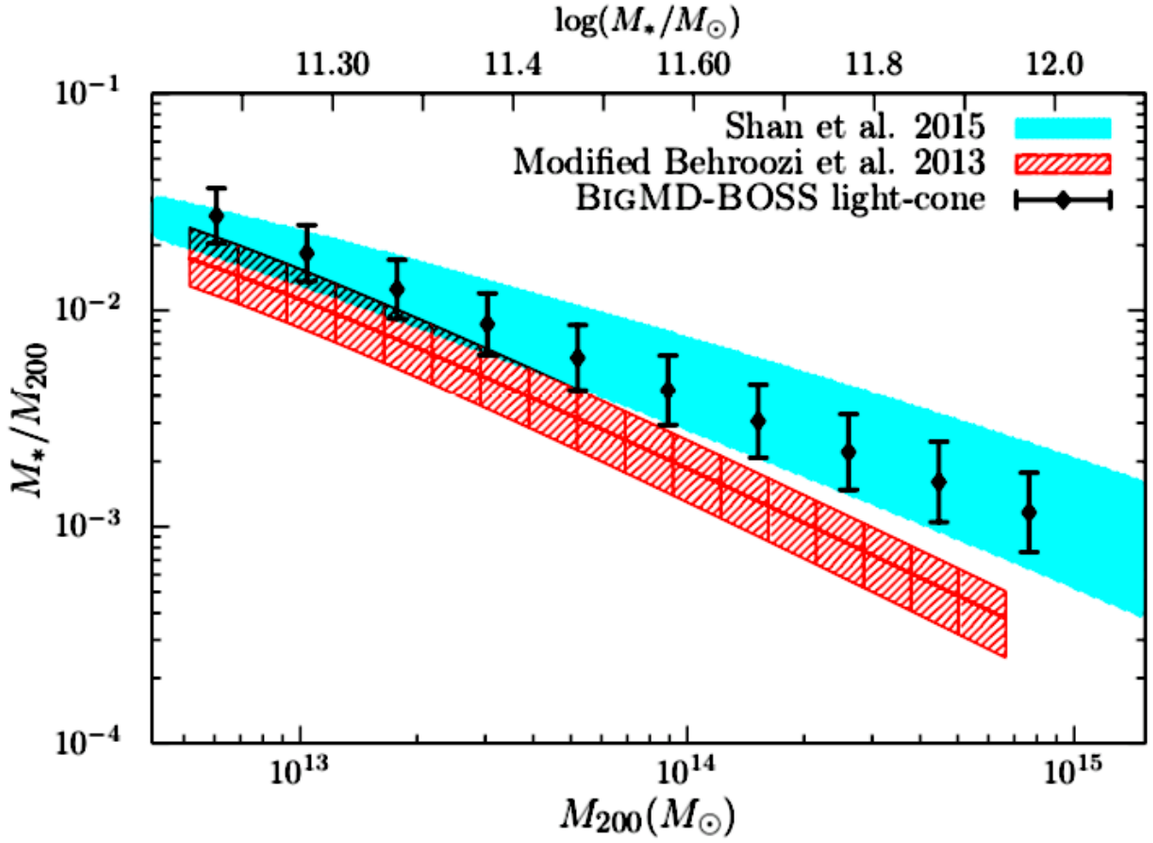

Figure 13. Stellar-to-halo mass ratio. The shaded blue area represents the best fit of the stellar to halo mass relation measured using weak lensing in the CFHT Stripe 82 Survey (Shan et al. 2015). The red area represent previous HAM result from Behroozi et al. 2013c. The analysis in Behroozi et al. (2013c) was modified using the Planck cosmology parameters and changing the definition of the halo mass. Black dots are the prediction from the HAM - BigMD-BOSS light-cone. Differences between our model and Behroozi et al. 2013c. are mainly due to the SMF adopted in both works. Scatter between M_{200} and M_* is similar between the

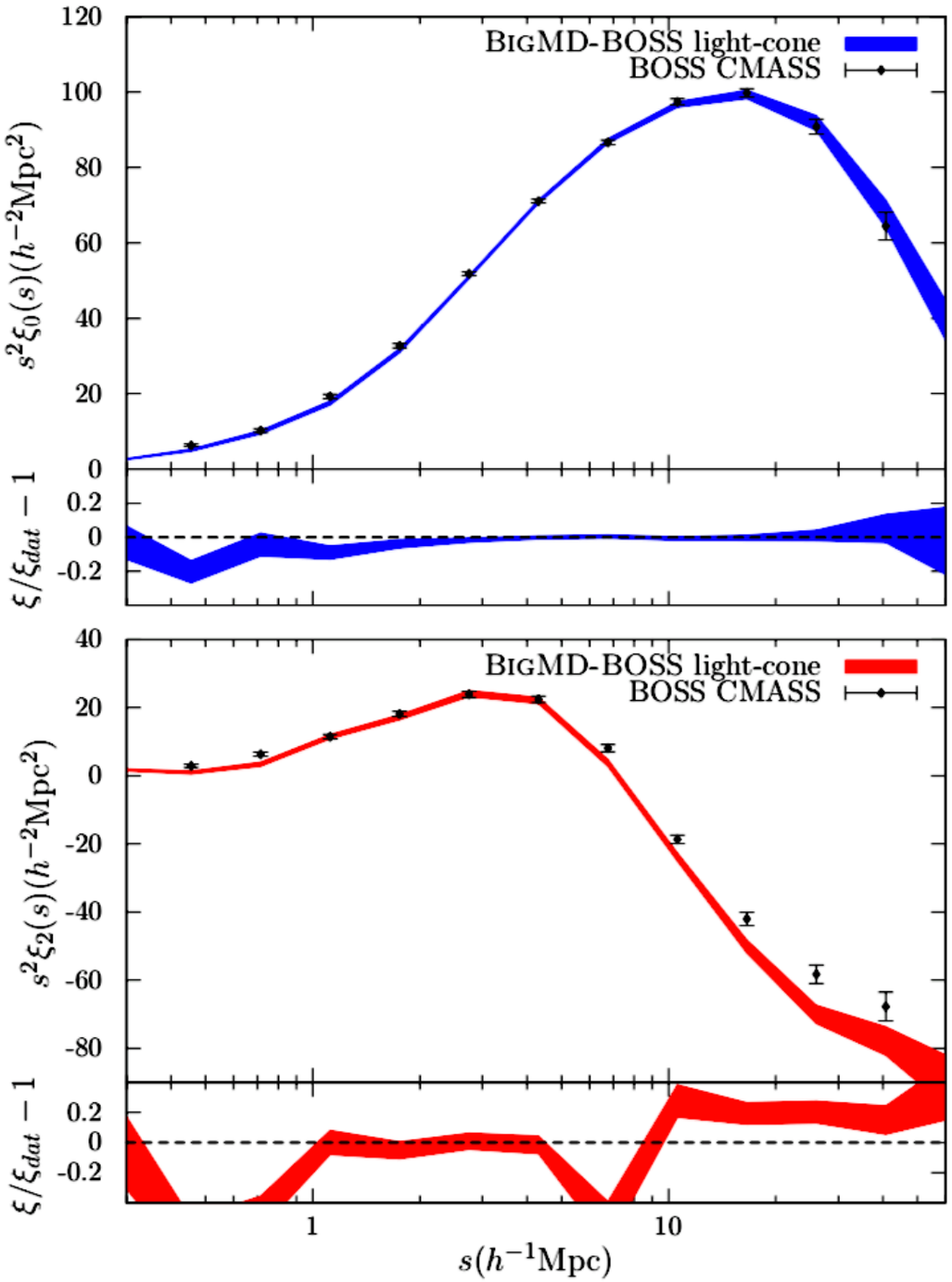

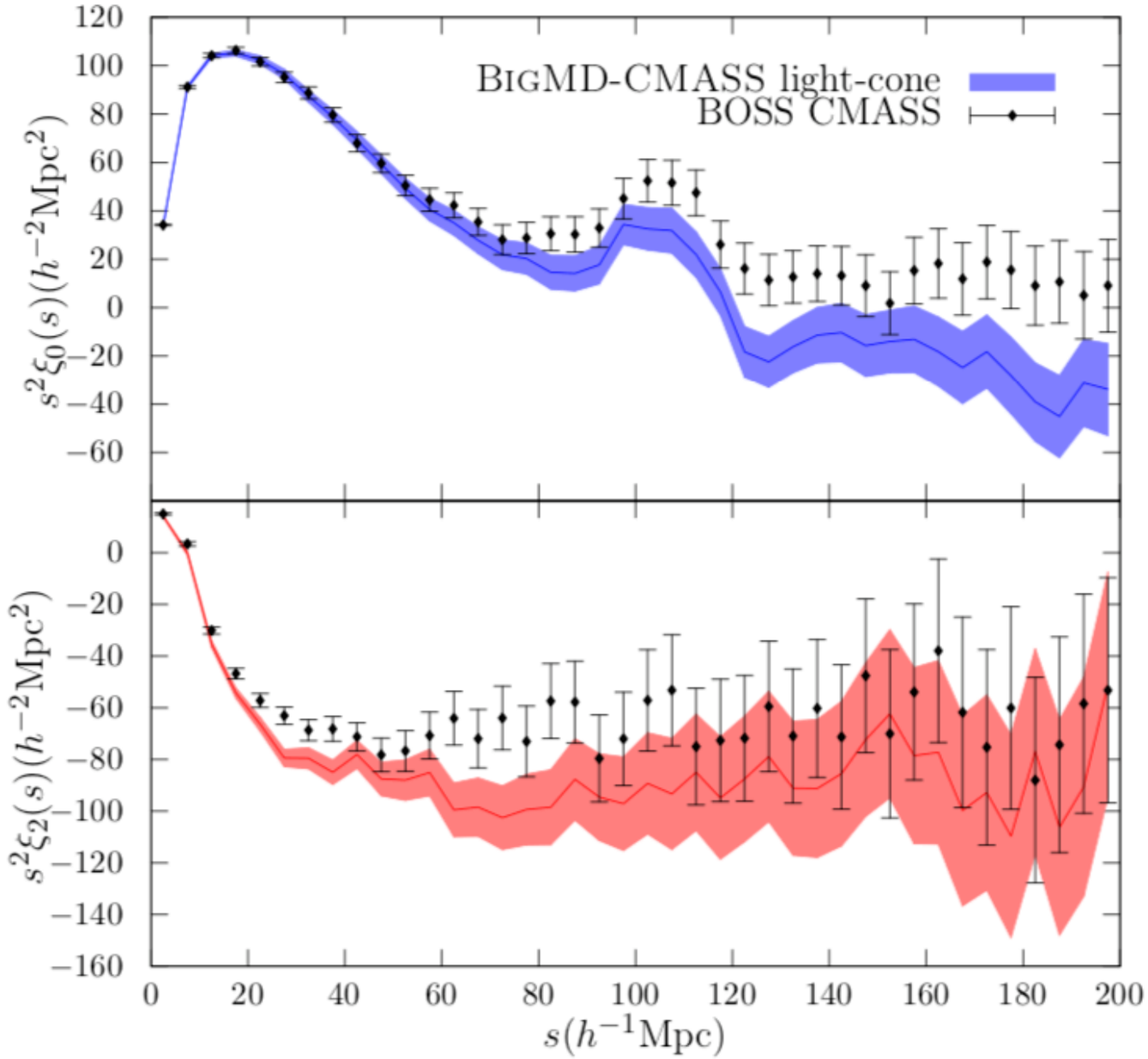

Figure 8. *Top panel*: Monopole in Redshift-space from CMASS DR12 sample (black points). The shaded area represents the modelling of the monopole using the BigMD-BOSS light-cone. *Bottom panel*: Quadrupole in Redshift-space from CMASS DR12 sample compared with the theoretical prediction from the BigMD-BOSS light-cone. Error bars were computed using MD-PATCHY mocks. Small panels show the ratio between the model and the observed data. Fitting of the monopole is performed between 2 h^{-1} Mpc and 30 h^{-1} Mpc. The observed monopole is in good agreement with our model for scales larger that 2 h^{-1} Mpc. However, the quadrupole shows tensions with observations for scales < 1 h^{-1} Mpc and $5 >$ h^{-1} Mpc.

Assembly bias: limitations on abundance matching

Clustering of dark-matter halos and galaxies depend not only on halo mass but also on their accretion history.

CMASS sample of 300,000 LRGs at z=0.5-0.6.

Spectra provide Star Formation Rates . These are early-type (not forming stars) galaxies.

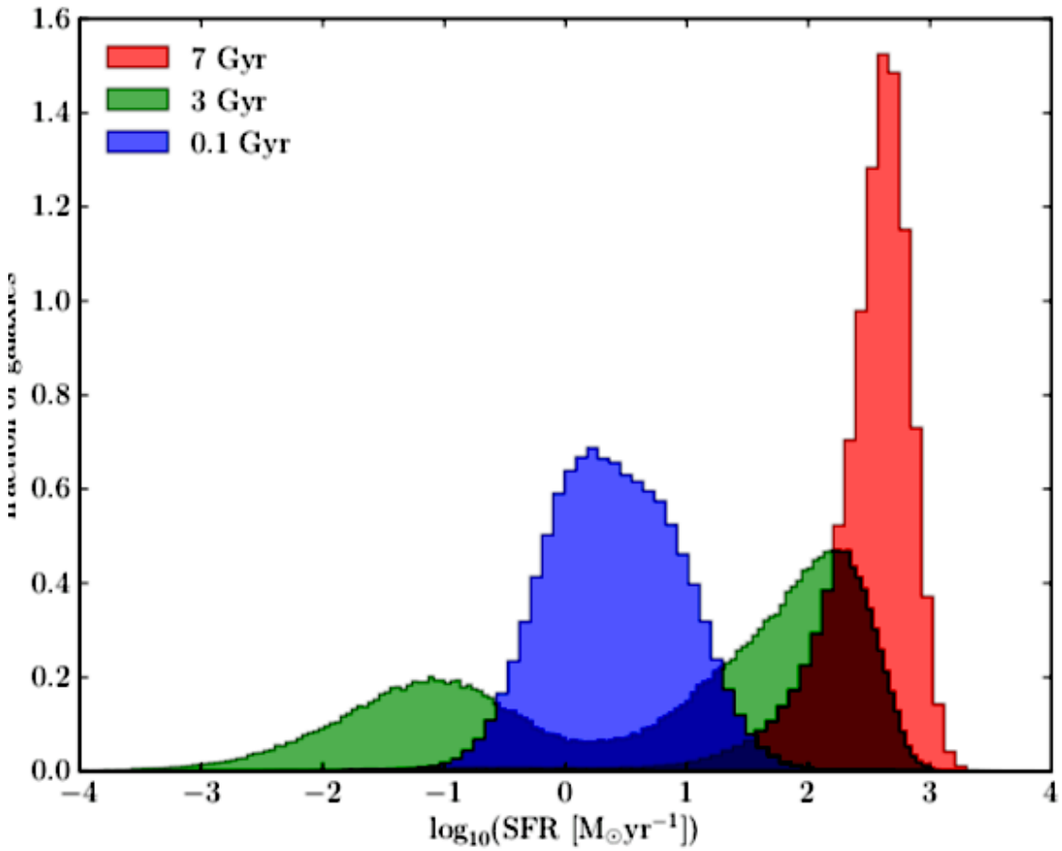

The distribution of the logarithm of the SFR, in units of M⊙ yr−1, in three different snapshots of galaxy-frame look-back time, centered at 0.1, 3 and 7 Gyr, respectively. The distributions have been normalized to unit area.

the fast- and slow-growing LRG populations, are defined using the SFR at 3 Gyr galaxy-frame look-back time:

$\mathrm{SFR3} < 2\ \mathrm{M}_{\odot} yr^{-1}$ (fast-growing)

$\mathrm{SFR3} \geq 2\ \mathrm{M}_{\odot} yr^{-1}$ (slow-growing)

Montero-Dorta et al 2018

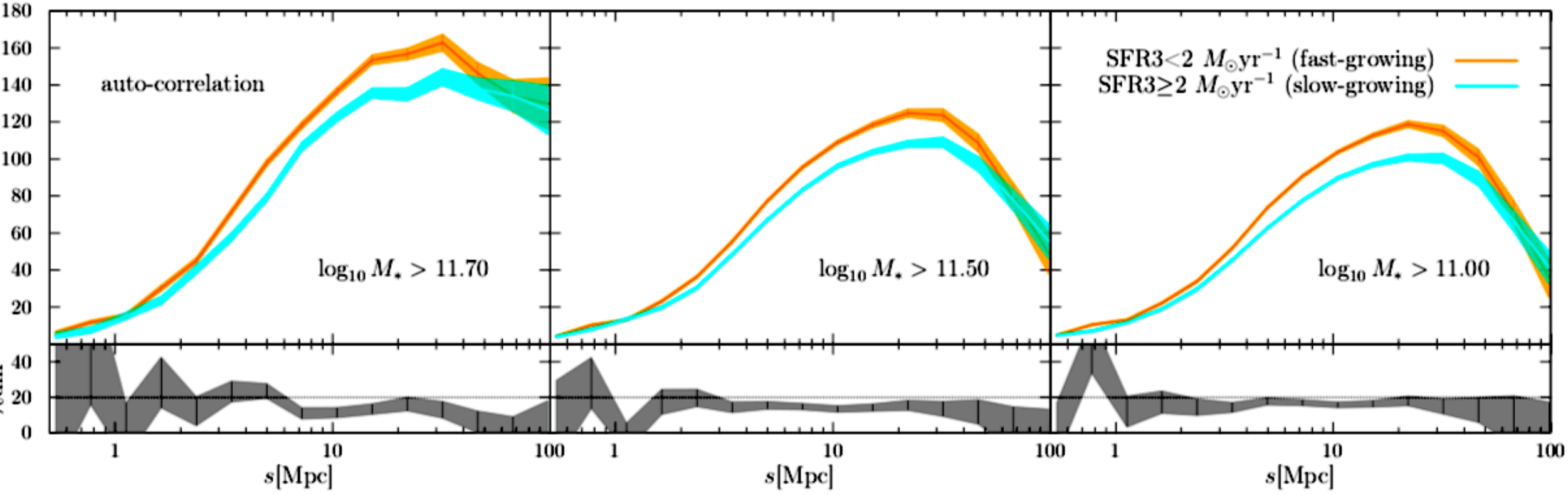

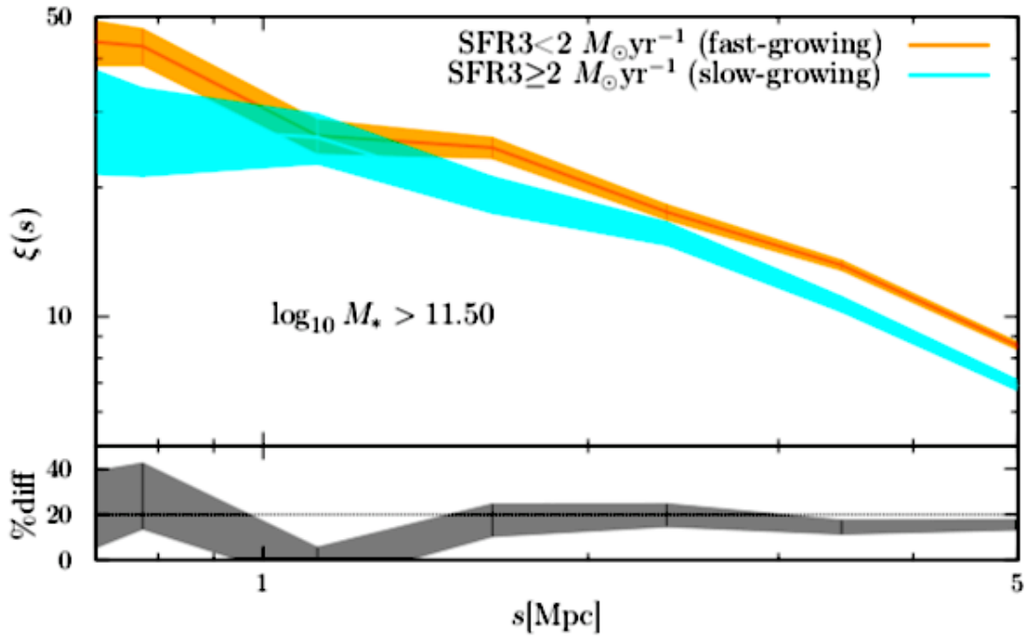

Figure 5. The monopole of the redshift-space 2D correlation function (auto-correlation) on small scales for the fast- and the slow-growing LRG populations in the cumulative stellar mass bin $\log_{10} M_*(M_\odot) > 11.5$. Error bars are computed using a set of BOSS DR12 MultiDark-Patchy mocks. Fast-growing LRGs have $\sim 20\%$ stronger clustering amplitude on scales $s \gtrsim 1$ Mpc. In-

Hearin et al. 2013, 2015

Two properties of halos (1) Vmax and (2) redshift at with halo stops (or significantly reduces) gas cooling.

1. $z_{\rm char}$: The first epoch at which halo mass exceeds $10^{12}h^{-1}M_{\odot}$. For halos that never attain this mass $z_{\rm char} = 0$.

2. $z_{\rm acc}$: For subhalos, $z_{\rm acc}$ is the epoch after which the object always remains a subhalo. For host halos, $z_{\rm acc} = 0$.

3 $z_{\rm form}$: Using the methods of Wechsler et al. (2002) we identify the redshift at which the halo transitions from the fast- to slow-accretion regime, as this is the epoch after which dark matter ceases to accrete onto the halo's central region.

From these three characteristic epochs we define the redshift of starvation:

$$z_{\rm starve} \equiv {\rm Max}\left\{z_{\rm acc}, z_{\rm char}, z_{\rm form}\right\}. \qquad (2)$$

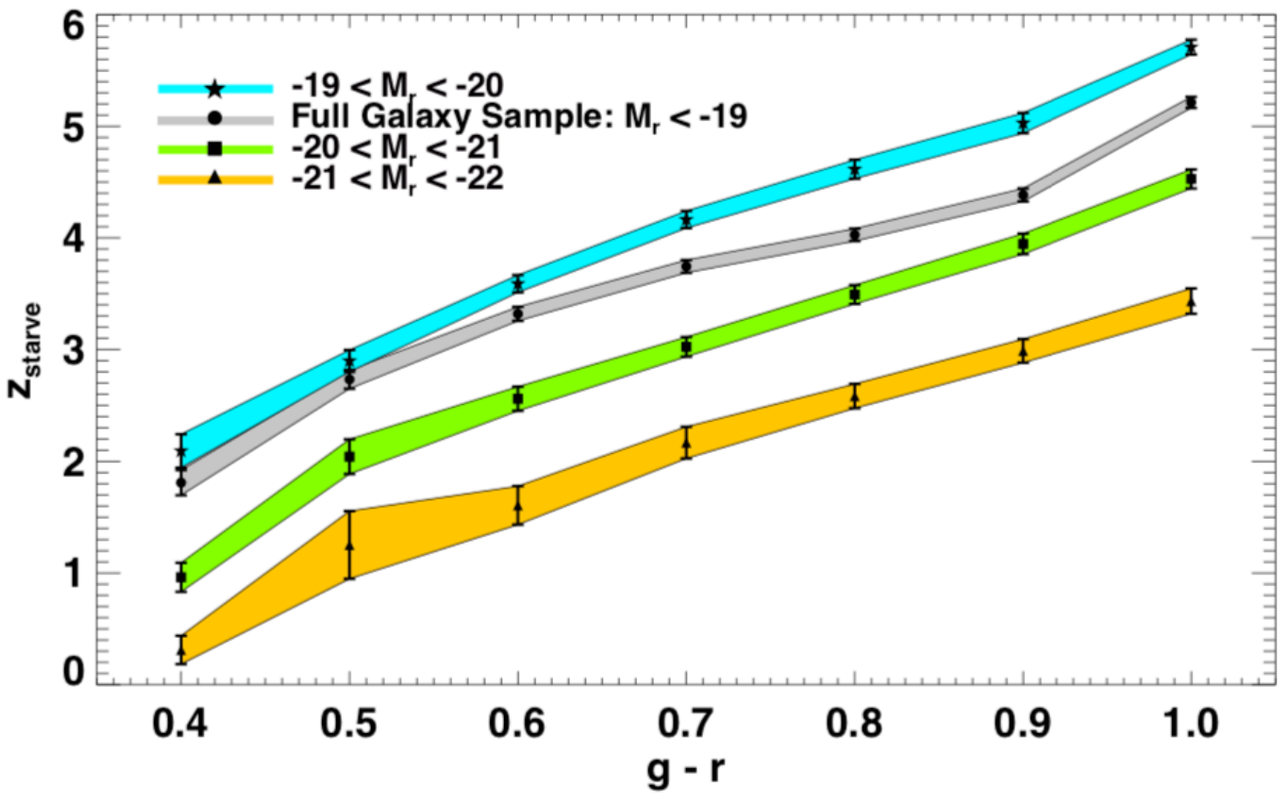

Luminosity- and color-dependent clustering as predicted by our age distribution matching formalism. Left Column: The luminosity-binned projected 2PCF predicted by our model (black solid curves) against the clustering exhibited by SDSS galaxies. Right Column: In bins of luminosity, we plot the projected 2PCF of red (blue) mock galaxies with red (blue) solid curves. Red, filled (blue, open) points show the clustering of red (blue) SDSS galaxies.